Guilherme Coutinho

M00684745

Middlesex University London

Middlesex University

Faculty of Science and Technology

Biomedical Engineering

BMS3676: Principles of Medical Engineering

Project A

Approaches to acquiring air flow rate and undertake Computational Fluid Dynamics using SolidWorks Flow Simulation

Module Leader's: Dr Andrew Tizzard

Jan 2021

Abstract

Finding the vital capacity is an important clinical diagnose that helps doctors to diagnose diseases related to obstruction of the lungs, such as asthma, bronchitis, emphysema, and others lung complications. Air is a low-density gas and very volatile in nature. To predict its behaviour is a difficult task that requires a long list of hard calculations. However, studying this phenomenon is a crucial step to engineers, due to the many applications that rely on it. On this report we are going to study and simulate the behaviour of air flow in a Lilly head pneumotachograph spirometer and create different 3d models using *Solidworks Flow Simulation* to obtain results of the air fluid dynamic. We will also compare the input volume flow rate of the simulation with the results of an analytic expression and study how the volume flow rate relates with the pressure drop.

1. Introduction

The spirometer is an instrument used for measuring lung volume capacity, also known as vital capacity in the medical field. The first spirometer was originally invented in 1840 by John Hutchinson, an English surgeon that, through a calibrated bucket placed upside down in water, was able to effectively measure the volume of the exhaled air from fully inflated lungs. Nowadays there are more different methods available for measuring this vital capacity, the most frequently used methods are the pneumotachograph, turbine, ultrasound, and a hot wire anemometer.

The respiratory system is a necessary part of the human body since all living cells in body need oxygen and produce carbon dioxide. Besides this fundamental action of exchanging gases, the respiratory system is also responsible for other functions such as controlling the Ph of the body, phonation, olfactory and protection from microorganism. The lungs are the main organs of the respiratory system and the most voluminous organ in all body. The right lung is divided into three lobes and the left in two, and these are then subdivided into ten and nine lobules, respectively. Here the lobules further divided originating the bronchopulmonary segments that are partially separated by a connective tissue where the ventilation happens by the bronchiole. When the respiration takes place the lungs get contracted or expanded. This happens

due to the movement of the muscles of respiration, being the main one the diaphragm, that forces air to move and creates air pressure between lung and the outside environment. During ventilation, an existence of a gradient pressure is formed between the outside and the alveoli. The air flows from the alveoli to the outside and equally in the opposite direction. The physiological principles of this gradient flow can be described in the following equation:

$$F = \frac{P1-P2}{R} \quad (1)$$

Where *F* is flow of air, *P1* and *P2* are pressure points and *R* is the resistance to the air flow.

This difference in pressures is what causes the air to move between the two points so when the pressure in a certain point (*P1*) is bigger than in other point (*P2*), the air moves from *P1* to *P2*. So during inspiration, a positive gradient pressure is created between the exterior and the alveoli, creating an atmospheric pressure bigger than the pressure in the alveoli, that results in the entering of air through the lower airways into the bronchioles in direction to the alveoli and reverse for expiration. This constant reverse of gradient pressures is called respiration and is what causes the diffusion of the gases to the blood. In this process the oxygen (O2) is replaced by carbon dioxide (CO2) by the osmotic pressure. When air enters the lungs by a low pressure, it forces the O2 in the air to defund into the terminal pulmonary arteries capillaries, resulting in carbon dioxide to diffuse into the alveoli, due to the difference in partial pressures.

The goal of the spirometry test is to measure the pulmonary function. This normally is done with the help of one instrument called spirometer that can measure the air volume and velocity. The goal of the instrument is to register four types of readings regarding the vital capacity: 1. The current amount of volume during inspiration and expiration during normal breathing process (average volume of 500 ml); 2. The maximum total volume during inspiration (about 3000 ml); 3. The maximum total volume during expiration (about 1100 ml) and 4. The residual volume meaning the remaining volume of air that is kept in the breading areas after total expiration (about 1200ml). These measurements are then used to diagnose the patients by comparing to the normal parameters of regular vital capacity (VC), Forced vital capacity (FVC) and Forced expiratory volume (FEV) (Seeley, Stephens and Tate, 2003).

The Lilly head pneumotachograph spirometer has a unique way of measuring the pulmonary function using a phenomenon known in physics as Venturi effect. The spirometer is composed by 5 components: two bells shaped heads, a meshing grid, a hose tube, a nose clipper, and a spirometer pod transducer connected to a computer. To measure the air flow rate the Lilly spirometer uses a porous membrane located in the middle of the spirometer that when the patient blows on the device it forces the air fluid to flow through the wire mesh porous membrane creating a pressure decrease and velocity increase which is known as Venturi effect. The spirometer then measures the pressure difference before and after the known resistance and transmits this value to the spirometer pod that converts them to an analogue input and filters random noise.

1.1. Mathematical principles of fluid mechanics

Fluid mechanics is the study of the fluid behaviour (liquids, gases, blood) under specific static and dynamics loads. This study is a branch that arises from continuous mechanics, where the kinematics and mechanical behaviours of material are modelled as continuous mass rather than discrete particles. In our model we are trying to measure the fluid flow across the spirometer, and this is described by the conservation equations for mass, momentum, and energy, commonly solved with the Navier-Stokes equations (4).

Another important equation commonly used when dealing with fluid mechanics is Bernoulli's equation, that tells us about the continuity of a fluid in a vessel and it can be used for measuring the amount of fluid flow in a closed vessel. This is very useful to solve the air flow across Lilly spirometer as this equation describes the relationship between pressure, fluid velocity, and height at different points and its sum remains unchanged.

$$P\,A\ + \frac{1}{2}\,\rho\,v^2\,\mathrm{A} + \rho\,g\,h\,A = \mathrm{C} \tag{2}$$

Where *P* is pressure, *A* is for the cross-sectional area, *ρ* represents the fluids density and *v* is equals to its velocity; the letter *g* represents the gravity acceleration and *h* the height; *C* it is a constant present by the laws of conservation of energy were the total amount of energy inside the Lilly's head is always constant.

The next set of equations used by the spirometer is the Darcy's law, that describes

the behaviour of the fluid flow through a porous medium. This equation that can be derived from the Navier-Stokes equations analysis of the permeability of a medium by its viscosity and pressure over a distance (Whitaker, *S. Flow in porous media*).

$$Q = -KA * \frac{dh}{dL} \tag{3}$$

In this equation *Q* is the rate of the fluid flow, *K* is the hydraulic conductivity, *A* is the cross-sectional area, and *dh/dL* indicates the hydraulic gradient.

Finally, the Navier-stokes equations are a set of equations very often used in fluids mechanics to determine the velocity vector field that applies to a fluid. They arise from the application of Newton's second law in a combination with fluid stress and a pressure term. These equations, that can be derived from the basic conservation and continuity equations, applied to the properties of fluids, requires specifying the stress tensor in terms of the properties of the flow. This stress tensor is often divided in two terms: the volumetric stress tensor, which tends to change the volume of the body, and the stress deviator that deals with the deformation of the body. These tensors are three-dimensional arrays that expresses relationship among three vectors and are represented by the *del* operator (∇). The following equation shows the general form of the equation assuming for an incompressible fluid (Gibiansky).

$$\rho\left(\frac{\sigma \mathrm{V}}{\sigma \mathrm{t}} + V * \nabla \mathrm{V}\right) = -\nabla \mathrm{P} + \mathrm{u}\nabla^2 V + F \tag{4}$$

On the left-hand side of the equation is the force on each particle, and states that the force is composed by three terms:

- $-\nabla P$: A pressure forces term, also known as volumetric stress tensor, that presses against itself and keeps it from shrinking in volume.
- $u\nabla^2 V$: A stress term knows as stress deviator, responsible for the turbulence and viscosity of the fluid that results from the friction and shear stress.
- *F*: the force term which is acting in every single fluid particle.

2. Methods

In this study we applied three different approaches, based on the *Solidworks* CFD Flow simulation study, to check upon the impacts of the pressure drop across different

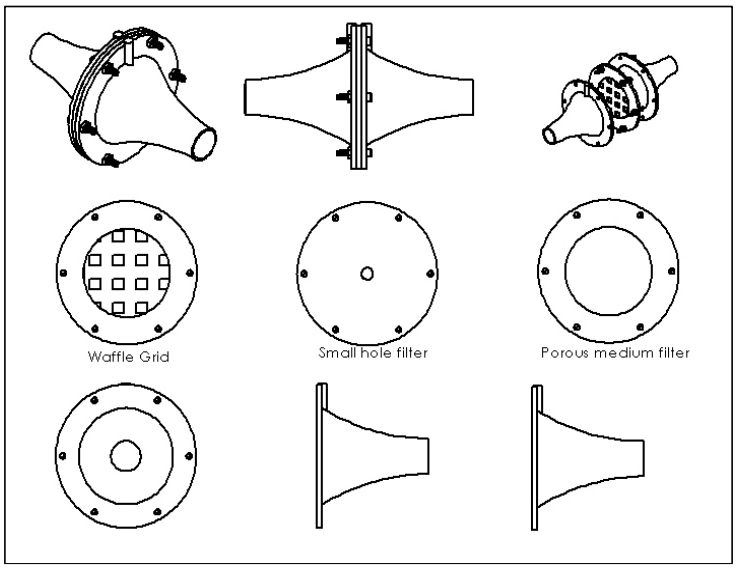

Figure 1: *Solidworks* drawings of the components of the Spirometer

resistances. In the first approach we simulated the flow through a waffle shape grid, with the square holes with dimensions of 9.8 x 9.17 in a diameter of 74mm (Appendix A). In the second one we used a recreation resistance of the real mesh metal grid using the properties of porous medium with a porosity of 0.775. In the third approach we used a small hole filter with 10mm of diameter. The shape of the models can be seen in Figure 1.

In all the three approaches we used the equation goal in the flow simulation, to determine the pressure drop of the spirometers. This was done by utilising the surface goal of the average pressure on both sides of the filter and then subtracting it. The spirometer was 190 mm long and the cross-section area of the spirometer inner cavity was composed by a 74 mm diameter. The total amount of volume, for the model of the spirometer and its filters, was of $0.1522\ m^3$ and the total number of cells used in the CFD analysis were about 72361. The mesh in the simulation used the dimensionality of pressure and stress with the basic dimensions of 500 in the number of X cells, 10 in the Y number of cells and 10 in Z number of cells. The boundaries conditions used for the inlet volume flow was the same in all the models, $0.01\ m^3/s$, $0.01033\ m^3/s$, $0.02\ m^3/s$ and $0.03\ m^3/s$ on the left interior face (LID1) in reference to axis X, and

no fully developed flow. For the outflow conditions we used an environmental pressure of 10250 Pa in the right interior face (LID2).

The reason why CFD or any other computational simulation are so useful for this type of problems is due to its fast properties of analyse and accuracy solving complex mechanicals systems that normally involve a long list of unsolvable differential equations calculations. This tool offers a more visual and reliable way to achieve the outcomes and permits the engineer to test and verify multiple solutions of their construction models, allowing him to create reasonable approximation of the results, draw conclusions and vary statistics. Besides these, real-life tests are often expensive, and time consuming and so simulations provides a much safer way to achieve the outcomes correctly. The application of this analysis in medicine has also contributed to the study and understanding of the human body, with the possibility to test and analyse particular aspects of the anatomy of the patient and derive conclusions in detail without a direct approach. This has been done extensively in the orthopaedic area were the application of prothesis require a rigours and personalized study of the patient's anatomy before the implementation (Easley *et al* 2007).

CDF analysis ways of calculation are based on finite volume method, which is essentially a method for solving partial differential equations such as the Navier-stokes equations. The way it does this is to divide the domain into many small control volumes and integrate the conservation law into them. This method, beside solving accurately flow problems, also helps the software to deal better with memory issues and high Reynolds number turbulent flows (Tu *et al* 2018). For the properties of the porous medium derived from the Darcy's laws we found that the software CFD simulation uses instead the following equation to determine the effective porosity of the porous medium:

$$K = (A * V + B)/\rho \tag{4}$$

Where V is the fluid velocity, A and B are constants and ρ is the air density. Here, only A and B are specified, since V and ρ are calculated (Technical Reference *Solidworks* Flow Simulation, 2017).

The effectiveness of porous medium in CFD simulations has been proven on a published paper in 2010 that reported results for mosquito woven screens. There, they

compared a simulation of a realistic porous slab and a porous medium model, and concluded that pressure drops could accurately be determined by a porous medium model and that this approach would reduce computation time about 20 times (Teitel and Shklyar 1998).

In the model of the porous medium filter we designed a plate with a 74mm diameter where we applied a new porous material, in the *Engineering Database.* The properties used in this new porous material was *A* value of 7000000 Kg/m^4 and *B* value of 7506.6 Kg/sm^3. We then set the permeability to unidirectional and for the resistance calculation we choose dependency on velocity. To preserve the energy of the flow fluid we set the heat conductivity off on the porous matrix. These properties were used as an attempt to keep the minimum turbulence in the fluid and to conserve the continuity laws inside the spirometer (Tutorials *Solidworks* Flow Simulation, 2017).

To confirm the continuity of the fluid inside the spirometer we made an analytical expression of the Bernoulli's principles to equate the volume flow rate calculation. In Figure 2, we can see how we achieve the theoretical volume flow rate (Q) of the air inside the spirometer and how it relates to the pressure drop.

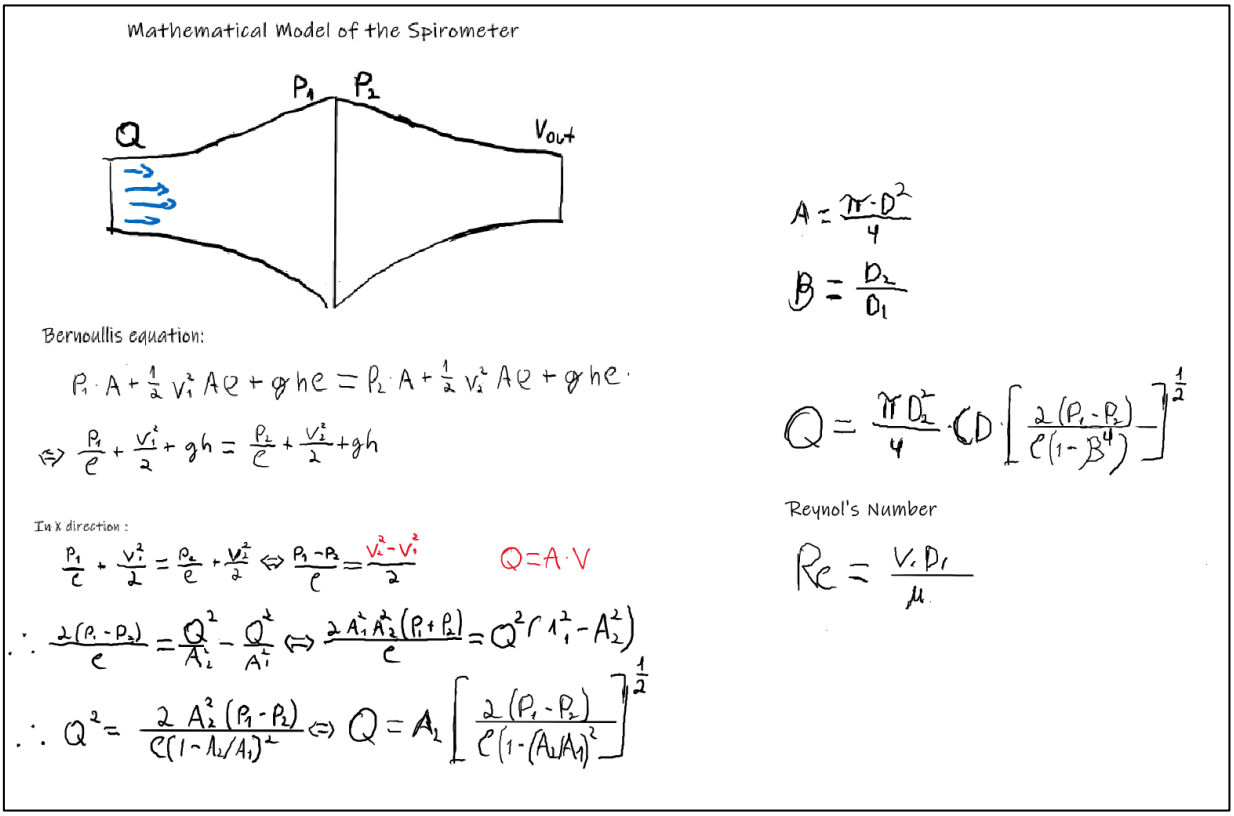

Figure 2: Mathematical model of the Lilly Venturi Spirometer System. On this figure we see the equation of flow rate volume used to find the flow rate. This is an analytic expression from the Bernoulli's equation.

Here, the *A* is the cross-section area , *B* is the beta ratio of the orifice, *CD* is the Coefficient of discharge and *Q* is the volume flow rate.

3. Results

The results obtained in the CFD spirometer simulation vary significantly from the predicted in the analytical approach in Figure 2. On the first model, the waffle shape grid shows in colours four different pressures generated with the flow rate of $0.01\ m^3/s$. Here, the data from the equation goal showed an average in total pressure drop of 57 (Pa) for $0.01\ m^3/s$, 61 (Pa) for $0.01033\ m^3/s$, 222 (Pa) for $0.02\ m^3/s$ and 548 (Pa) for $0.03\ m^3/s$. We also noticed that this type of filter caused some turbulence in the fluid (Figure 3); this can be seen by the mixed green and vortices formation on the right side showed by the streamlines.

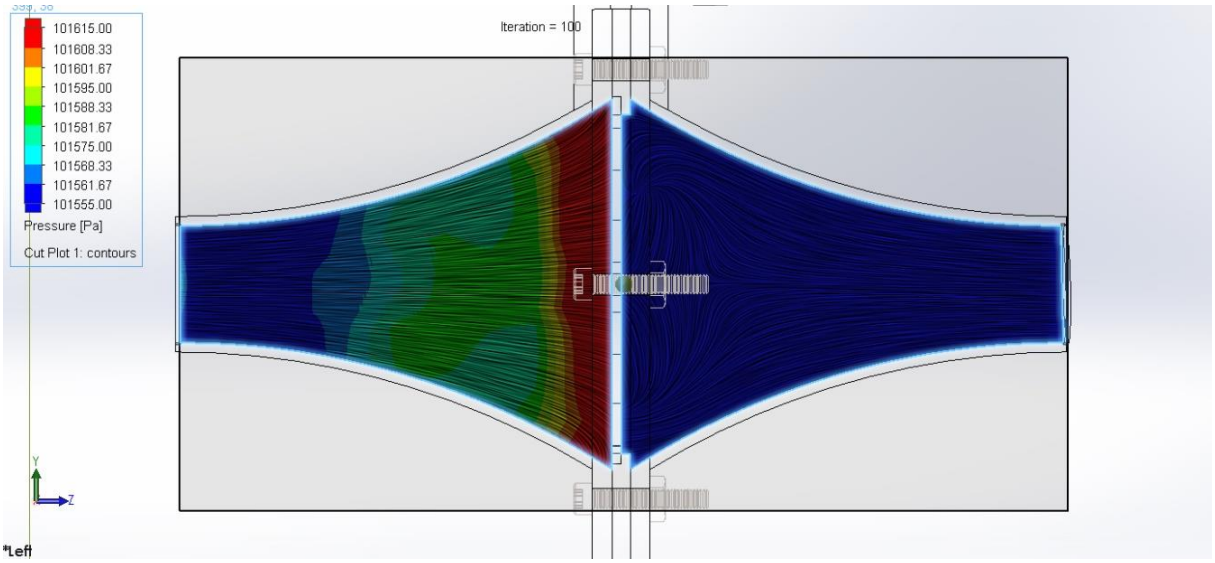

Figure 3: CFD study of the spirometer in the waffle grid filter. The middle part shows a high amount of pressure in yellow and red regions and low air pressure in the blue regions near the extremities. We can also see the streamlines that illustrate the motion of the air.

On porous medium CFD simulation the results showed a more active pressure drop, with a visual pronounced high pressure on left-hand side showed by the colour Red and low pressure towards the filter and right-hand side showed by the colour blue. However, the motion of the flow appears less turbulent and more laminar. The data from the equation goal of the average total pressure drop was 835 (Pa) for the $0.01\ m^3/s$, 1482 (Pa) for $0.01033\ m^3/s$, 4369 (Pa) for $0.02\ m^3/s$ and 12467 (Pa) for $0.03\ m^3/s$ (Figure 4).

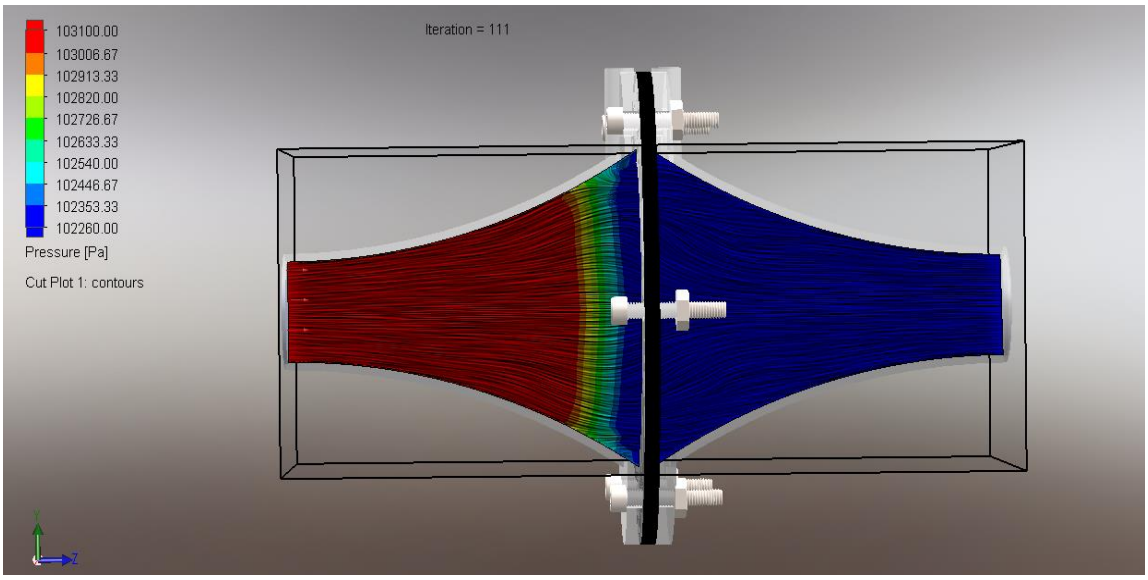

Figure 4: CFD in the Porous medium properties. We find that the effective porosity of the porous medium is seen to generated high pressure on the left side in red and progressive pressure drop towards the filter.

Finally, on the small hole filter simulation we noticed the highest pressure drop in all the simulations, with an average value of pressure in P1 with 794178 (Pa) and P2 $1.77x10^7$(Pa) for 0.01 flow rate, this resulted in a tremendous pressure drop of 974368 (Pa) and turbulent flow with formation of vortices on both sides (Figure 5). In the middle, during the cross of the filter on the right side we find a small area where there is some transition to low pressure.

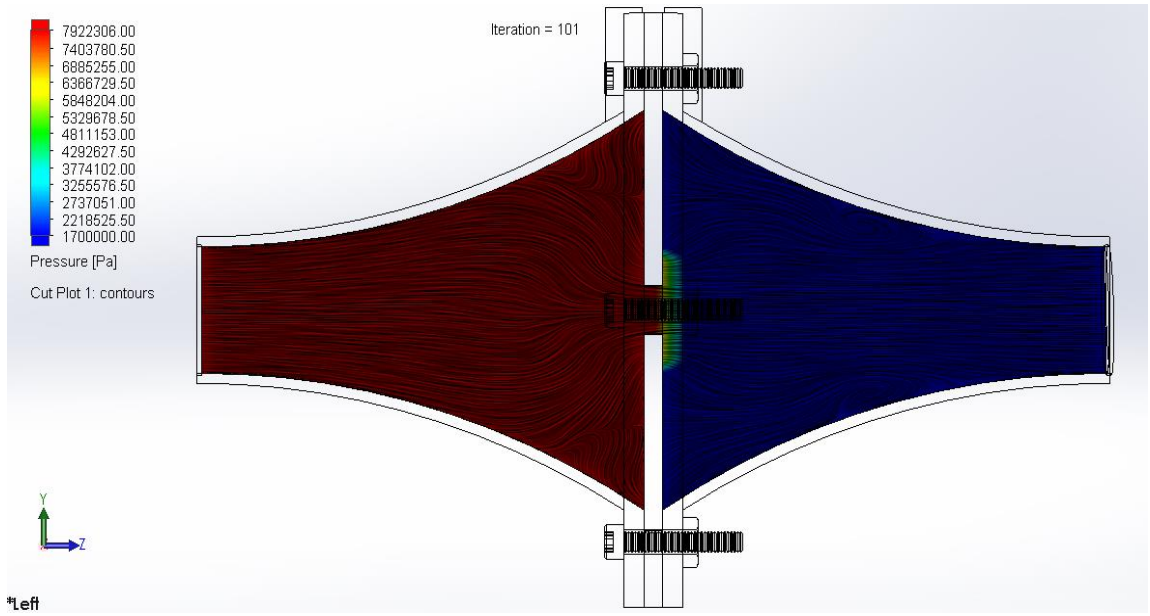

Figure 5: Venturi effect in the small hole filter. On right side we see a high air pressure in red and on the left low pressure in blue. We also see a small area near where the pressure expands, and turbulent flow on both sides

Table 1 shows the results of the volume flow rate calculated from the analytical expression equated from the Bernoulli's equations (Figure 2) and the Coefficient of discharged (Cd) that shows the ratio between the theoretical and the volume flow rate used in the simulation.

Table 1: Results from Bernoulli's equations and its respective Cd

Q(m^3/s) Simulation Cd = 1	**Theoretical Q(m^3/s) Porous medium**	**Theoretical Q(m^3/s) Waffle shape grid**	**Theoretical Q(m^3/s) hole filter**
0.01	0.0081	0.0021	0.8755
0.01033	0.0108	0.0022	0.8997
0.02	0.0185	0.0042	1.7349
0.03	0.0313	0.0065	2.6078
Coefficient of discharged			
Cd Porous medium		**Cd Waffle shape grid**	**Cd Hole filter**
1.2342		4.7027	0.0114
0.9566		4.7109	0.0115
1.0790		4.7273	0.0115
0.9580		4.5706	0.0115

From the analytical expression the results of the calculations of the theorical volume flow rate were found to be near the input used *Q* in the CFD simulation of the porous medium simulation with the *Cd* being very near to one. However, the *Cd* for the waffle was very high and for the hole filter very small.

Figure 6, 7 and 8 show the relationship of pressure drop as function of the volume flow rate (Q) from the porous medium, waffle filter and the hole filter. Figure 9 shows a graphic of the pressure drop function of length caused in the hole filter.

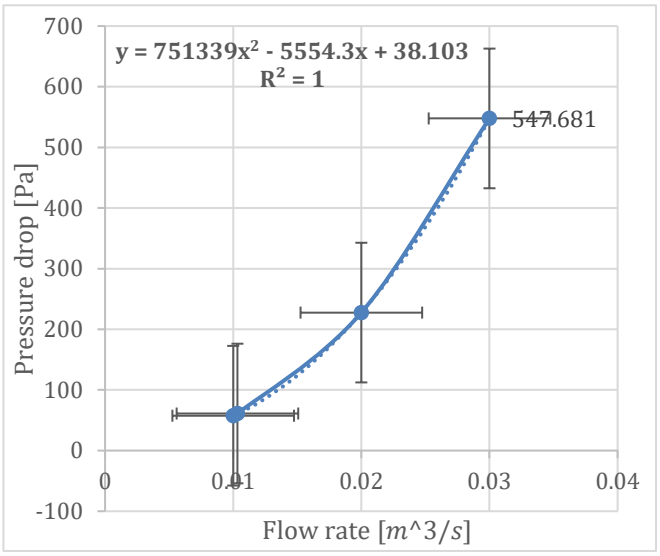

Figure 6: Pressure drop as function of flow rate (porous medium)

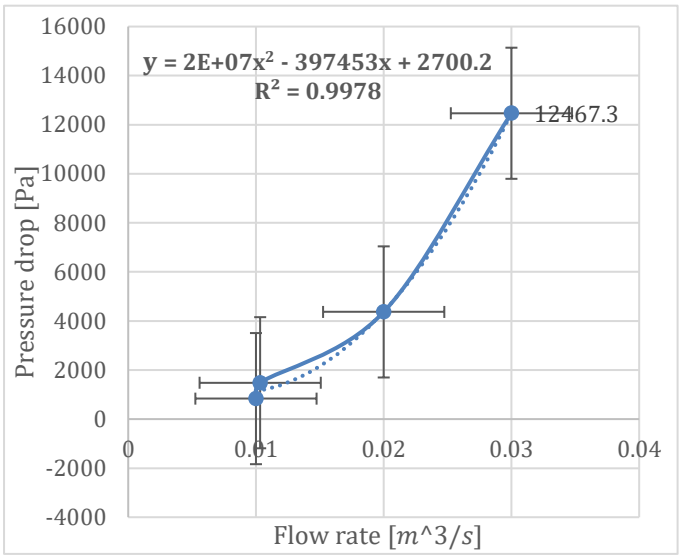

Figure 7: Pressure drop as function of flow rate (Waffle grid)

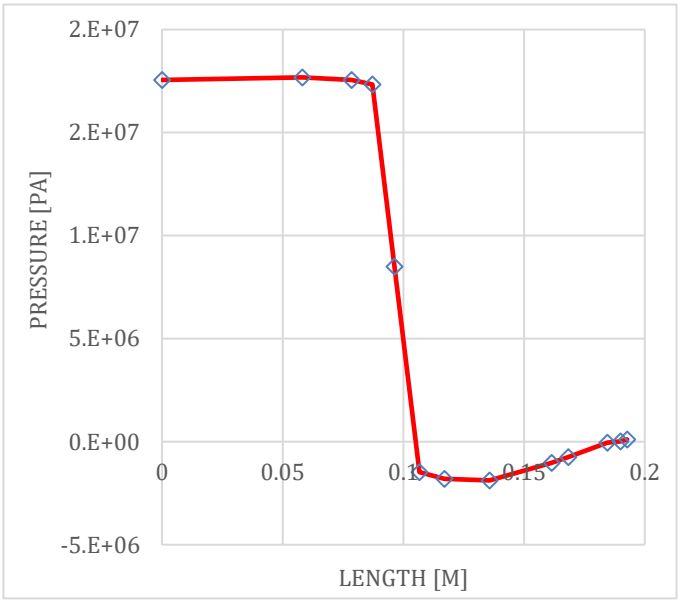

Figure 9: Pressure drop as function of flow rate (hole)

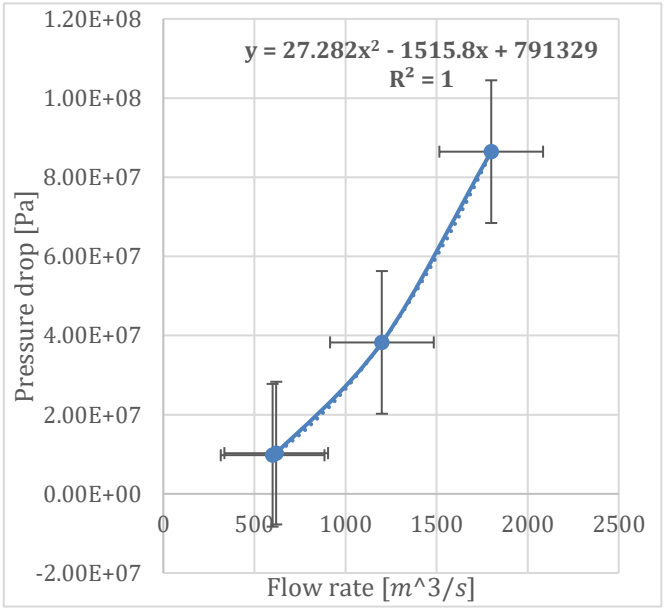

Figure 8: Pressure drop as function of flow rate (hole)

4. Discussion and Conclusions

CFD represents an effective fluid simulation for analysis of fluid mechanics; however, due to our limitation of the large porosity of waffle filter model, did not contribute for an honest comparison with the porous medium. The pressure drop generated by the porous medium showed that the stimulation results are very approximated for the analytical approach based on the Bernoulli's equations (2) and Figure 2. In agreement with model's prediction, the porous medium simulation had a higher discharged confidence (Cd) which resulted in a lower Reynolds number (Re) and therefore a more laminar flow (DigitalCommons *et al* 2011). Our models suggested that the high pressure drop side effects of CFD simulation resulted in a more turbulent flow (Figure 5) (Teitel and Shklyar 1998). However, this is not necessarily true. Due to the waffle grid model the pressure drop was much lower, but the turbulence was higher than in the porous medium. In addition, it was unclear if the hole filter model served as beneficial or detrimental to the outcome, due to its unrealistic nature that cause a tremendous pressure drop with high Re and incoherent Cd.

While this study provides quantitative results on the effects of Pressure drop in a CFD simulation, that would be difficult to achieve experimentally, because there are two important limitations in the models that should be noted. First, we used a bad realistic representation of the real mesh grid that had its porosity in order of less than 1 mm. Second, that the use of porous medium depends on the Darcy's law or a variation of it, that incorporates an empirical determined flow resistance in the region of the model defined as porosity. This causes to not describe the state of flow within an individual pore and not consider the actual curvilinear path of the fluid particle. Our goal was to develop a simplified estimation of the volume flow rate (Q) that could be derived directly from the Bernoulli's equations by evaluating the pressure drop (P2-P1) in an environment that had present laminar flow and neglecting air compressive properties, maintaining constant the volume flow properties. This means that the volume flow rate used in the simulation had to be the approximated to the analytical solution. This simplified estimation has an error of several limitations as previous discussed and showed by the standard deviation in Figure 7. However, given the large area where the volume of air went (Figure 4) the error is relatively small, especially on the high flow rates simulations. Nonetheless, our model of the Lilly head pneumotachograph spirometer represents a good attempt to characterize the volume

flow rate function as the pressure drop of a real spirometer because of the similar properties that the porous medium recreates.

The increase in the volume flow rate seemed to generate a direct proportionality to pressure drop in all of the filter models that were applied. This relation if due to the second derivative of the velocity which is equal to the division of flow rate by the area which will produce in both Reynolds number and discharged confident to increase and decrease, respectively (Figure 2). These numerical predictions have been verified in numerous experimental preparations demonstrating the difference between CFD through a porous medium, design of realist porous slabs and FEA simulations on the ability to accurately represent fluids behaviour.

In conclusion, analyses of the behaviours of fluids are complicated due to its volatile nature and our limited capacity of prediction the response to the surrounding environment as well as its natural ability to disperse. However, computational simulation methods help us to have a better control over the laws of physics and understand better these incredible complex systems.

5. References

2017.TECHNICAL REFERENCE SOLIDWORKS FLOW SIMULATION. Dassault Systems, p.52.

2017.TUTORIALS SOLIDWORKS FLOW SIMULATION. Dassault Systems, p.A3-4

Andrew Gibiansky *Fluid Dynamics: The Navier-Stokes Equations Classical Mechanics*

DigitalCommons, All Graduate Theses and Dissertions, *Utah State University* Hollingshead C L 2011 Discharge Coefficient Performance of Venturi, Standard Concentric Orifice Plate, V-Cone, and Wedge Flow Meters at Small Reynolds Numbers

Easley S K, Pal S, Tomaszewski P R, Petrella A J, Rullkoetter P J and Laz P J 2007 Finite element-based probabilistic analysis tool for orthopaedic applications *Comput. Methods Programs Biomed.* **85** 32–40

Seeley, R., Stephens, T. and Tate, P., 2003. Anatomy and Physiology. 6th ed. McGraw-Hill Science Engineering, pp.826-864.

Teitel M and Shklyar A 1998 Pressure drop across insect-proof screens *Trans. Am. Soc. Agric. Eng.* **41** 1829–34

Tu J, Yeoh G-H and Liu C 2018 Introduction *Computational Fluid Dynamics* (Elsevier) pp 1–31

Appendix A : Technical Drawings of solidworks models used in the CFD simulation